Talanta 227 (2021) 122161

Contents lists available at ScienceDirect

Talanta

journal homepage: www.elsevier.com/locate/talanta

# Molecular diagnostic of toxigenic *Corynebacterium diphtheriae* strain by DNA sensor potentially suitable for electrochemical point-of-care diagnostic

Kasper Marchlewicz [a], Iga Ostrowska [a], Sławomir Oszwałdowski [b], Aleksandra Zasada [c], Robert Ziółkowski [a,*], Elżbieta Malinowska [a,d]

[a] Warsaw University of Technology, Faculty of Chemistry, The Chair of Medical Biotechnology, Noakowskiego 3, 00-664, Warsaw, Poland
[b] Faculty of Chemistry, The Chair of Analytical Chemistry, Warsaw University of Technology, 00-664, Warsaw, Poland
[c] National Institute of Public Health - National Institute of Hygiene, Department of Sera and Vaccines Evaluation, Chocimska 24, 00-791, Warsaw, Poland
[d] CEZAMAT PW, Poleczki 19, 02-822, Warsaw, Poland

ARTICLE INFO

*Keywords:*
Electrochemistry
DNA
Diphtheria diagnostics
Diethyldithiocarbamate

ABSTRACT

The presented study is focused on the development of electrochemical genosensor for detection of *tox* gene fragment of toxigenic *Corynebacterium diphtheriae* strain. Together with our previous studies it fulfils the whole procedure for fast and accurate diagnostic of diphtheria at its early stage of infection with the use of electrochemical methods. The developed DNA sensor potentially can be used in more sophisticated portable device. After the electrochemical stem-loop probe structure optimization the conditions for real asymmetric PCR (aPCR) product detection were selected. As was shown it was crucial to optimize the magnesium and organic solvent concentrations in detection buffer. Under optimal conditions it was possible to selectively detect as low as 20.8 nM of complementary stand in 5 min or 0.5 nM in 30 min with sensitivity of 12.81 and 0.24 $1 \cdot \mu M^{-1}$ respectively. The unspecific biosensor response was elucidated with the use of new electrode blocking agent, diethyldithiocarbamate. Its application in electrochemical genosensors lead to significant higher current values and the biosensor response even in conditions with magnesium ion depletion. The developed biosensor selectivity was examined using samples containing genetic material originated from a number of non-target bacterial species which potentially can be present in the human upper respiratory tract.

## 1. Introduction

The uncontrollable spread of pathogens can lead to serious threads for human health and life [1]. As could be observed during the recent pandemics of COVID-19, Swine or Spanish flu also the global markets can suffer from such an circumstances [2,3]. That is why the early stage infection detection and fast introduction of the appropriate preventive measures are the central issues for public health, environment protection and, in exceptional situations, also in the prevention for the global financial recession. Moreover, because of the climate change, globalization, mass people migration or the anti-vaccination movements, it is certain that new infectious threats or an old ones will continue to (re-) emerge and spread. This makes research and development of tools dedicated to rapid diagnosis of infections an indispensable part of the fight against them [4–7]. The method of choice, for any early stage infection identification, seem to be detection of DNA or RNA specific for a given pathogen and, if possible, also its antigens. This can be clearly observed during the recent COVID-19 pandemic and related WHO recommendations [8]. Although traditional methods are sensitive and can give equally qualitative and quantitative information of the investigated microorganisms, they are severely restricted by the assay time, the cost and place of the analysis and by the skilled personnel availability [9–12]. New technologies using microfluidic platforms with disposable or reusable biosensors have emerged, aiming to match Affordable, Sensitive, Specific, User-friendly, Rapid and Robust, Equipment free, Deliverable to end users (ASSURED) criteria [13]. Because of it portability, compact dimensions and low operational cost the detection elements used in such an devices usually are equipped with electrochemical transducers [14]. This guarantee fast response times, low detection limits and flexibility in detection mechanisms used [14].

The aim of the presented study is the further insight into diphtheria early stage diagnostic based on electrochemical approach. This highly infectious and potentially lethal human disease, caused by toxigenic *Corynebacterium diphtheria* strains, characterizes extremely short

* Corresponding author.
*E-mail address:* robert.ziolkowski@pw.edu.pl (R. Ziółkowski).

https://doi.org/10.1016/j.talanta.2021.122161
Received 5 November 2020; Received in revised form 21 January 2021; Accepted 26 January 2021
Available online 8 February 2021

incubation period (2–5 days) [7]. Since the introduction of vaccination against diphtheria, in the 1940s, the infections seemed to be controlled in developed countries. However, according to ECDC data, the confirmed diphtheria cases in EU/EEA increased over three times from 2011 to 2015 [15]. Diphtheria is endemic in many countries of Asia, the South Pacific, the Middle East, and Eastern Europe and since 2011 outbreaks were recorded in Indonesia, Thailand, Laos, South Africa, Sudan, and Pakistan [16]. Between 2012 and 2016 almost 28400 cases of diphtheria were recorded worldwide [17]. In addition, the diphtheria cases were described in asylum seekers in Europe [18,19]. This makes diphtheria one of the potentially most serious public health problem [20,21]. Rapid and accurate tests are of high value because clinical diagnosis of toxin-producing strains of *Corynebacterium diphtheria* is not easy and might be confused with other causes, such as streptococcal sore throat or tonsillitis [22]. This time consuming diagnosis is based on isolating *C. diphtheriae* and testing the isolate for toxin production by the Elek test, an in vitro immunoprecipitation (immunodiffusion) assay. To identify *Corynebacterium diphtheriae* also other techniques can be considered, such as polymerase chain reaction (PCR) or matrix assisted laser desorption/ionization-time of flight mass spectrometry (MALDI--TOF). However they do not confirm toxin production by the potentially toxigenic *Corynebacterium* strains and are considered supplemental [7]. There are special recommendations for *Corynebacterium* species isolation, staining, and toxigenicity confirmation, what with the use of traditional procedures could last even a several days. These procedures are also severely restricted by the place of the analysis [23]. The diphtheria antitoxin, the protein which neutralize the bacterial lethal toxin, is not easily available in many countries and it takes time till it can be shipped to the medical facility. That is why of special significance are the methods which allow for simplifying and shortening of the above diagnostics procedures [24]. The commercially available kits and systems are dedicated only to identification of *Corynebacteria* spp., but there are no for full diphtheria toxigenicity confirmation [23]. One of the possible solution for above restrictions are electrochemical sensors which could be used as detection elements in more advanced Point-of-Care (POC) devices. To date for fast, electrochemical based diphtheria diagnosis we developed (i) electrochemical immunosensors for detection of toxin (toxoid) produced by *Corynebacterium diphtheria* [25,26], (ii) evaluated the influence of the swab type used for sample collection on the results obtained in toxoid/antibody or PCR reactions during *Corynebacterium diphtheria* diagnosis [27], (iii) developed miniaturized, microfluidic device dedicated to amplification of 107 nucleotide fragment of *tox* gene (coding diphtheria toxin) in asymmetric PCR reaction in 15 min [28]. However to accomplish the full electrochemical diagnostics, which fulfils the ASSURED criteria, also the detection of amplified *tox* gene fragment is indispensable.

The presented study is dedicated to development of the electrochemical DNA biosensor and conditions for detection of single stranded *tox* gene fragment amplified in asymmetric PCR reaction. After investigation of the effects of different factors (probe sequence and its second order structure, temperature, magnesium ion concentration, addition of dimethyl sulfoxide) on the sensor response, the real samples were analyzed. The selectivity of the developed biosensor was examined with the samples where genetic material was originated from a number of non-target bacterial species which potentially can be present in the human upper respiratory tract. Also the short descriptions of nucleic acid isolation and amplification methods used by us and suitable for resource limited areas are mentioned.

## 2. Materials and Methods

### 2.1. Equipment

Voltammetric measurement (cyclic voltammetry (CV), square-wave voltammetry (SWV) and alternate current voltammetry (ACV) were performed using CHI 660A and CHI 1040A electrochemical workstation (CH Instruments, USA). The experiments were conducted with a three electrode system consisting of a gold disk electrode (GDE) (CHInstruments, USA), an Ag/AgCl/1.0 mol $L^{-1}$ KCl reference electrode (Mineral, Poland) and a gold wire as an auxiliary electrode (Sigma Aldrich, Germany) or with the use of AC1.W1.R2 and AC1P.W1.R2 3-electrode transducers (BVT, Czech Republic). Cyclic voltammetry was executed at 0.1 V/s scan rate, square-wave voltammetry and alternate current voltammetry were performed at a pulse amplitude of 25 mV, an increment of 4 mV and different frequencies (from 15Hz to 300 Hz). For experiments performed in elevated temperature the peltier-cooled incubator IPP30 from Memmert (Germany) was used. DNA amplification was performed with Mastercycler AG 22331 thermocycler (Eppendorf, Germany) and visualized after electrophoresis (Hoefer, USA) with UV transilluminator.

### 2.2. Reagents

All chemicals and reagents were of analytical reagent grade and used as received, without further purification. Concentrated HCl (36.5–38.0%), NaOH, NaCl, KCl, $K_3Fe(CN)_6$, $K_4Fe(CN)_6$, $KH_2PO_4$, 6-Mercapto-1-hexanol (MCH), sodium diethyldithiocarbamate trihydrate (DETC), Tris, Borate, EDTA, concentrated $H_2SO_4$ (95.0–98.0%), dimethyl sulfoxide were purchased from Sigma Aldrich Chemicals (Germany). $MgCl_2$ was purchased from Fluka Analytical (Germany). $H_2O_2$ was purchased from POCh (Poland). Acrylamide (AA), N,N'-methylenebisacrylamide (Bis), ammonium persulfate (APS), and N,N,N,N'-tetramethylethylenediamine (TEMED) were purchased from Bujno. Chem. (Poland). Alumina powders of grain size 1, 0.3 μm and 0.05 μm were purchased from Buehler (USA). Ready-to-use master mix for PCR containing Taq Polymerase, dNTPs and $MgCl_2$ in buffer: Hot- StarTaq Master Mix Kit was purchased from QIAGEN (Germany). Agarose was purchased from MP Biomedicals™ (USA). Primers for PCR were purchased from Oligo (Poland), electroactive probes were purchased from Metabion (Germany) and other unlabeled oligonucleotides were purchased from Genomed (Poland). For silica magnetic beads-based DNA extraction the MagJET Genomic DNA Kit was purchased from ThermoScientific (USA), and for filter paper-based DNA extraction the QIAGEN (Netherlands) reagents were used. The sequences used in the presented work, both with its symbol, are summarized below in Table 1.

### 2.3. Solutions

The following solutions were prepared: immobilization solution 1 M KH2PO4, pH 4.5; hybridization solution 10 mM Tris-HCl; 50 mM KCl; 2 mM MgCl2 pH 7,0; acidic piranha solution (H2O2/H2SO4; 3:1); $K_3Fe(CN)_6/K_4Fe(CN)_6$ in 20 mM PBS, pH 7.4. The pH was adjusted with 1 M NaOH or HCl water solution. Ten times concentrated Tris-Borate- EDTA (TBE) solution for electrophoresis (0.9 M Tris and Borate and 0.01 M of EDTA, pH 8.3). All solutions were prepared with Milli-Q water.

### 2.4. Receptor layer preparation procedure

Prior the biosensor preparation, the gold electrode was polished successively with alumina powder of grain sizes from 1 to 0.05 μm. Then the electrode was washed with water and sonicated for 15 min in demineralized water. Next, the piranha solution was dropped on the working gold disk electrode and incubated for about 5 min. After removing this solution, the electrode was washed again with demineralized water. Then it was scanned electrochemically (−0.5–1.7 V) in 1 M NaOH and 1 M H2SO4 until the CV characteristic for a clean gold was obtained. After washing the electrode with demineralized water and CV scanning in hybridization buffer in the potential range used in further experiments, the receptor layer preparation was started. First, the 0.2 μM solution of chosen electrochemical probe in immobilization solution was deposited on the electrode surface for 30 s. After that time the electrode was rinsed with immobilization buffer and left in 2 mM MCH

**Table 1**
Sequences used in presented work, their names and function. For electrochemical probes also their predicted stem and loop fragment lengths are given (AttoMB2 –blue methylene covalently attached to DNA probe).

| Name | Sequence | Function |
|---|---|---|
| *tox* gene fragment/ *cDNA/aPCR* | 5'- CAA TCA TCG TCA TAA TTT CCT TGT GTA CCA GAT TTT GGC TTT TGT ATA CCT TTT TGA ATG GAA TCT ACA TAA CCA GGT TTA GTC CCG TGG TAC GAA GAA AAG TTT TC -3' | Target for electrochemical biosensor. cDNA – commercial product, HPLC purified aPCR – real asymmetric PCR product |
| Short-toxF | 5'- CAA TCA TCG TCA TAA TTT CCT TGT GTA CC -3' | Starter for *tox* gen fragment amplification |
| WHO2 | 5'- GAA AAC TTT TCT TCG TAC CAC GGG ACT AA -3' | |
| TOX1 | 5' –thiol C6 - A tatacctt GAA AAC TTT TCT TCG TAC CAC GGG ACT AAA CCT GGT TAT GTA GAT TCC ATT CAA AAA GGT ATA – AttoMB2 - 3′ | Probe for electrochemical detection of *tox* gen fragment |
| TOX2 | 5' –thiol - A tatacc GAA AAC TTT TCT TCG TAC CAC GGG ACT AAA CCT GGT TAT GTA GAT TCC ATT CAA AAA GGT ATA – Atto MB2 -3′ | |
| TOX3 | 5' –thiol - A ggaatc GAA AAC TTT TCT TCG TAC CAC GGG ACT AAA CCT GGT TAT GTA GAT TCC – Atto MB2 -3′ | |
| TOX4 | 5' –thiol - A acataa GAA AAC TTT TCT TCG TAC CAC GGG ACT AAA CCT GGT TAT GT– Atto MB2 -3′ | |

solution in immobilization buffer for overnight. Then it was rinsed several times with immobilization buffer and water and left in hybridization solution for approximately 10 min. Afterwards further measurement were conducted.

### 2.5. The tox gene fragment amplification in standard PCR mode

The PCR reaction (standard PCR reaction) was performed in a final volume of 20 μl. The reaction mixture contained: 6.5 μL of sterile deionized water; 10 μl Hot Start Taq 2x Master Mix [Hot Start Taq DNA Polymerase, dNTPs, $MgCl_2$, KCl]; 0.5 μl of 10 mM of each primer; 2.5 μl of template DNA. The amplification reaction was carried out in a Mastercycler AG 22331 thermocycler (Eppendorf) under the following conditions: 95 °C for 15 min, then 35 cycles: 94 °C for 45 s, 60 °C for 45 s, and 72 °C for 45 s, the last step 72 °C, 5 min. The amplification products were separated on a 2% agarose gel (MP Biomedicals) in 1xTBE buffer.

### 2.6. The tox gene fragment amplification in asymmetric PCR mode (aPCR)

The asymmetric PCR reaction was performed in a final volume of 40 μl. The reaction mixture contained: 14.75 μL of sterile deionized water; 20 μl Hot Start Taq 2x Master Mix [Hot Start Taq DNA Polymerase, dNTPs, $MgCl_2$, KCl], 1 μl 10 mM F primer and 0.25 μl 10 mM R primer; 4 μl of template DNA. The amplification reaction was carried out in a Mastercycler AG 22331 thermocycler (Eppendorf) under the following conditions: 95 °C for 15 min, then 35 cycles: 94 °C for 45 s, 60 °C for 45 s and 72 °C for 45 s, the last step 72 °C, 10 min. The amplification products were separated on a 2% agarose gel (MP Biomedicals) in 1xTBE buffer (Fig. 6). The DNA template for the PCR reaction was a DNA template isolated from the *Corynebacterium diphtheriae* PW8 strain (*tox* +, *dtxR* +). The amplification product was obtained by applying forward and reverse primers complementary to the expected sequence, at different concentrations. The forward to reverse primer ratio used was 1:4, one of which was completely depleted during the first amplification cycles. In the following cycles, the excess primer elongated, giving the appropriate asymmetric PCR product - single strand DNA (ssDNA) of a specific length.

### 2.7. Bacterial strains and DNA extraction

Bacterial strains, the toxigenic and nontoxigenic *C. diphtheriae* and other bacterial species that might be present in the respiratory tract (Fig. 3 in supplementary material, SM) were cultured from freezing (−70 °C) on suitable culture media for each of the species: Columbia Agar with 5% Sheep Blood (COS) (Biomerieux), Common Agar (Bekton Dickinson), Heamophilus Chocolate Agar (Biomerieux) and incubated for 24 h at 37 °C. In the case of the *Heamophilus influenze* strain, incubation was carried out in an atmosphere of 5% $CO_2$. The next day, after checking the purity of the cultures obtained, the selected colony was passaged into the culture medium for the genetic material isolation and *tox* gene fragment amplification. DNA extraction was performed for 24 h bacterial cultures on the medium appropriate for the bacterial species by using DNeazy Blood and Tissue Kit (Qiagen, Germany) according to the manufacturer's instructions for Gram-positive and Gram-negative bacteria, respectively.

### 2.8. Silica magnetic beads-based DNA extraction

*Corynebacterium diphtheriae* cells resuspended in 0.87% NaCl to density 1 McF were used as a tested sample. A swab was placed in the suspension for a few seconds and then transferred to 300 μl of TE buffer, mixed for a few seconds and removed. The sample was incubated for 10 min at 96 °C. Next, 300 μl of lysis buffer B-1 (3 M guanidine hydrochloride; 0,2% Tween-20) were added and the sample was mixed by vortexing for 5–10 s. The sample was transferred to a tube prefilled with 400 μL of isopropanol and 25 μl of silica magnetic beads suspension (ThermoScientific). The tube was mixed by vortexing and placed on the magnetic rack for 2–3 min. Supernatant was removed using a pipette. The tube was removed from the magnetic rack, 800 μl of washing buffer (10 mM Tris HCl pH 8.0; 1 mM EDTA, 70% ethanol) were added, the tube was mixed by vortexing and placed on the magnetic rack for 2–3 min. Supernatant was removed using a pipette. The tube was removed from the magnetic rack, 150 μl of TE buffer were added, the tube was mixed by vortexing and incubated for 5 min at 72 °C with mixing occasionally. After incubation the tube was placed on the magnetic rack for 2–3 min and the supernatant containing extracted DNA was transferred to a new tube.

### 2.9. Filter paper-based DNA extraction

*Corynebacterium diphtheriae* cells resuspended in 0.87% NaCl to density 1 McF were used as a tested sample. A swab was placed in the suspension for a few seconds and then transferred to 300 μl of lysis buffer B-2 (20 mM Tris-Cl, pH 8,0, 2 mM sodium EDTA, 1,2% Triton X-100) with 50 μl of lysozyme (100 mg/ml), mixed for a few seconds and removed. The sample was incubated for 30 min at 37 °C. Then, 200 μl of AL buffer (QIAGEN) and 50 μl of proteinase K (20 mg/ml) were added, the sample was mixed by vigorous reverting the tube and incubated for 30 min at 56 °C. A piece of about 0.5 $cm^2$ of filter paper Watmann no. 2 was placed into the sample and incubated for 3 min at room temperature. Then the filter paper was transferred to a new tube containing 100 μl of TE buffer and mixed vigorously. The suspension contained extracted DNA.

### 2.10. DNA extraction using DNeazy Blood and Tissue Kit (Qiagen)

*Corynebacterium diphtheriae* cells resuspended in 0.87% NaCl to density 1 McF were used as a tested sample. A swab was placed in the suspension for a few seconds and then transferred to 200 μl of enzymatic

lysis buffer. The extraction was conducted according to the manufacturer's instruction for Gram-positive bacteria.

## 3. Results and discussion

The early stage identification of human infection with bacterial or virus agent is indispensable for fast introduction of appropriate preventive measures. This is especially important as the new (COVID-19) or treated as a past and forgeted infectious threats (plague [29]) (re-) emerge and spread.

To secure the operation simplicity, reagentless and reusable electrochemical detection of the *tox* gene fragment in real conditions, we decided to use as the probes the loop-and-stem "hairpin" DNA sequence. In this case the registered signal, biosensor response, depends only on the conformational changes of the probe after hybridization with complementary strand, amplified e.g. in asymmetric PCR reaction. The mechanism is based on the analysis of the distance between redox probe, tethered to DNA probe, and the electrode surface (Fig. 1). The biosensor response (signal change) is related to the spatial changes between ssDNA (Fig. 1A) probe and dsDNA (Fig. 1B).

As the complementary single stranded DNA recognition influence the distance between redox marker and electrode surface, it results in reduction of registered current intensity. The change in electrochemical signal is calculated according to Eq. (1):

$$\frac{I_0 - I}{I_0} \cdot 100\% \quad (1)$$

where: $I_0$ - current registered for receptor layer before hybridization step; I - current registered for receptor layer after hybridization.

Such an approach will eliminate, among others, the unspecific interactions present in other detection mechanisms, like free redox indicator added to the sample and its adsorption, electrostatic attraction or mixed interactions with biosensing elements present at the electrode surface [30–34].

The mentioned *tox* gene fragment (107 nucleotide long), amplified and detected in the sample taken from the patient, can be the indication of the infection with the potentially toxigenic *Corynebacterium* strain (only diphtheria toxin detection confirms strain toxigenicity). The gene itself encodes the diphtheria toxin which penetrates directly into the host cell and inhibits the multiple proteins synthesis which finally leads to the cell death. The lethal dose of this toxin for humans is about 0.1 μg per kg of body weight [35].

### 3.1. The electrochemical stem-loop probe sequence selection and cDNA detection

The first step of the electrochemical genosensor preparation was the selection of electrochemical probe sequence. Although examples of genosensors based on electrochemical stem-loop probes dedicated to detection of short, approximately 30 nucleotide long, DNA or RNA strands have been reported in the literature, there are no strict recommendations for the probe sequence designing for detection of longer nucleic acids strands, especially dedicated to real life applications. According to our previous findings [32] in presented studies the stem-loop probe architecture was based on the stems no longer than 7 bp (stems for three probes were of 6 bp and for one 7 bp long) and loops from 35 to 57 nucleotides (Table 2). The predicted most stable second order structures of the used sequences, together with their Gibbs energies, are shown in Table 2. There could be observed differences between the designed stem and loop lengths and the most stable second order structures adapted by the sequences.

As can be seen both second order structures and Gibbs free energies of the chosen stem-loops strongly depends on their sequences. In the biosensor construction as receptor probe first the TOX1 stem-loop was used (the highest second order structure stability from the investigated, ΔG -6.58 kcal $mol^{-1}$). The biosensor's receptor layer was prepared with the same procedure as in Ref. [32] and briefly described in experimental part. This allowed for the stem-loop spatial distribution at the electrode for efficient cDNA recognition process [32]. Before the cDNA recognition the sensor was conditioned in hybridization buffer till the signal stabilization (approximately 10–15 min). After that the HPLC purified cDNA detection was conducted. The analyte recognition process was carried out in the same hybridization buffer as in our previous studies (2 mM $MgCl_2$, 50 mM KCl, 10 mM Tris-HCl, pH 7) [32]. Such a buffer composition shows high similarity in ion concentrations to the PCR mix used in ssDNA fragment amplification (material part). Nonetheless as can be seen (Fig. 1A, supplementary material, SM) for 2 mM $Mg^{2+}$ this time no satisfactory results were obtained. Because the similar ion concentration in PCR MIX allowed for PCR product amplification in bulk solution (Fig. 1B-SM), it can be concluded that there are significant differences in ssDNA/ssDNA hybridization efficiency conducted in bulk solution (PCR reaction) and at solid–liquid interfacial (electrochemical biosensor). As these two environments (solution and surface) are substantially different also the significantly different effects influence the ssDNA/ssDNA recognition process: (i) steric hindrances of the receptors immobilized at the transducer surface which could influence the ssDNA/ssDNA hybridization, (ii) the stability of the second order structure of the electrochemical DNA stem-loop probe, (iii) the electrostatic repulsion between the analyte (phosphate moieties in ssDNA)

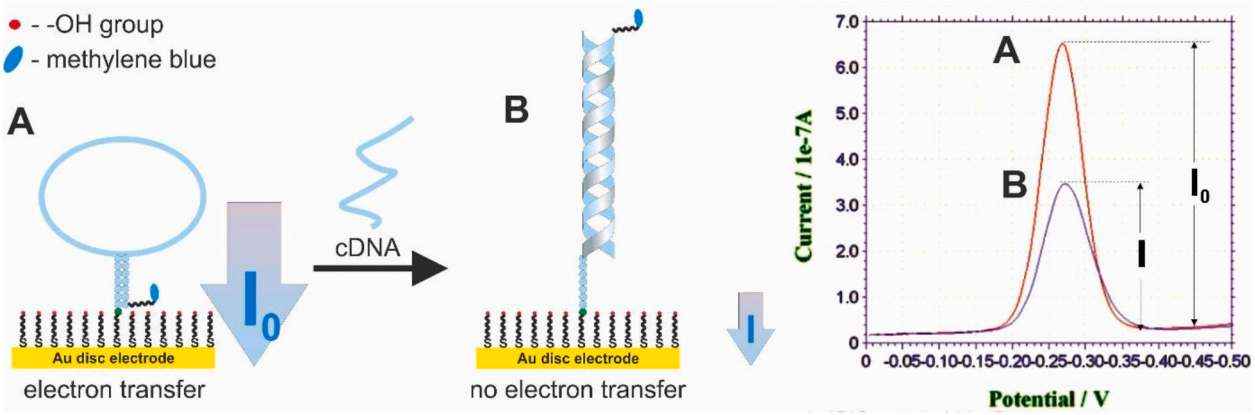


**Fig. 1.** Mechanism of electrochemical *tox* gene detection (A) a zipped stem-loop probe with redox marker in a small proximity to the electrode surface; (B) open stem-loop probe with redox marker in increased distance from electrode surface. The graph represents change in registered electrochemical signal before ($I_0$) and after (I) ssDNA hybridization.

**Table 2**
Influence of the electrochemical stem-loop probe sequence and their second order structures stability (predicted at the base of [36]) on the sensor response toward different cDNA concentrations ($n \geq 4$).

| Probe's second order structure of the lowest energy | Other 3 most stable second order structures | Sensor response for cDNA recognition for 5 and 30 minutes hybridization |
|---|---|---|
| TOX 1 / -6.58 [kcal·mol$^{-1}$]<br>Stem length: 7 bp<br>Loop length: 57 nucleotides<br>  | 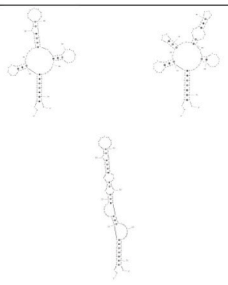 | 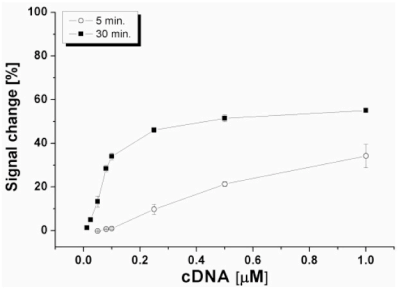 |
| TOX 2 / -4.79 [kcal·mol$^{-1}$]<br>Stem length: 6 bp<br>Loop length: 57 nucleotides<br>  | 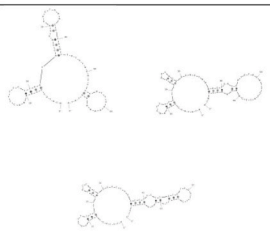 | 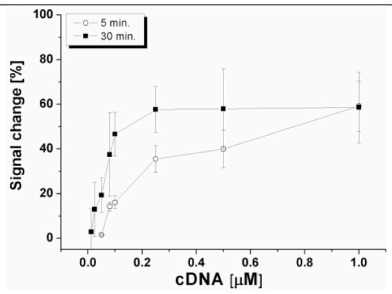 |
| TOX 3 / -5.58 [kcal·mol$^{-1}$]<br>Stem length: 6 bp<br>Loop length: 42 nucleotides<br> 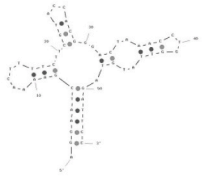 | 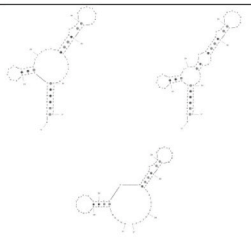 | 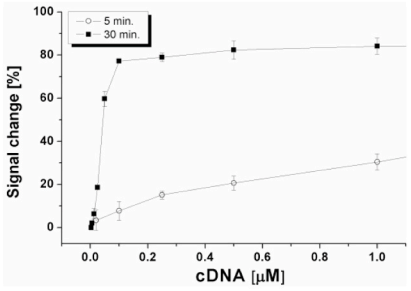 |
| TOX 4 / -6.45 [kcal·mol$^{-1}$]<br>Stem length: 6 bp<br>Loop length: 35 nucleotides<br>  |  | 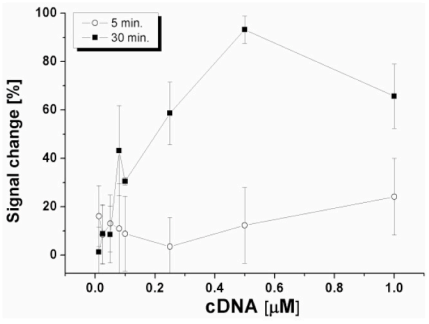 |

and the modified transducer surface (phosphate moieties in stem-loop probe and –OH groups of MCH). The first two of above was already investigated by us in Ref. [32], where the similar in length (82 nucleotide) single stranded PCR product was detected. Nonetheless, in the presented study both the chosen probe density nor the designed stem or loop lengths were not enough to obtain satisfactory biosensor response even for HPLC purified cDNA. This may result from the third of above effect, where ions present in hybridization buffer do not guarantee enough charge shielding in the case of investigated sequence, especially as the electrode blocking agent, the mercaptohexanol (MCH, –OH moiety possess partially negative charge and the same surface modified with mercaptohexanol) was used. Since magnesium ion characterizes with much more compact distribution around DNA duplex than other monovalent species [37] we optimized its concentration versus

potassium ion in the hybridization buffer. As shown in Fig. 1A-SM, the hybridization efficiency was significantly improved by increasing the concentration of magnesium ion in the hybridization buffer. Above this concentration the efficiency in stem-loop/cDNA interactions was gradually diminish due to increasing the standard deviation (for better view in Fig. 1A-SM only results for chosen magnesium ion concentrations were presented). Based on above results buffer containing 15 mM $Mg^{2+}$ was used for evaluation of the applicability of the chosen stem-loop probes sequences in commercially available HPLC purified 107 nucleotide length *tox* gene fragment detection (Table 2). For each of the analyzed stem-loop sequence the hybridization process with complementary strand (cDNA) was conducted for 5 and 30 min. As could be seen (Table 2) the registered dependence between biosensor response and cDNA concentration was significantly influenced by the probe sequence used as a receptor in the sensing layer (each of investigated sensors were prepared in the same manner). The clear relationship between sensor signal change and cDNA concentration could be observed only for probes TOX1 and TOX3, which predicted second order structures (Table 2. Stem-loop structure) were of the highest similarity to the typical form of zipped "hairpin". Comparing the biosensor's signal change registered for these two probes after the hybridization with cDNA, the significantly higher values were obtained for TOX3. This can be explained by the differences in the free Gibbs energy of these probes, TOX1 -6.58 [kcal·$mol^{-1}$] and TOX3 -5.58 [kcal·$mol^{-1}$], which results in different energies needed for breakage of their second order structures. In the case of TOX2 and TOX4 probes no satisfactory results were obtained. The response of the sensor with TOX2 probe was proportional to cDNA concentration, however high standard deviations of the results were observed. When TOX4 probe was used, except poor linear response, the registered standard deviations were also of significant value. This is most likely due to the fact that for these two probes no typical stem-loop probe architecture could be observed. Moreover, for TOX4 probe two separate peaks were registered (results not shown) which is highly undesired as potentially both peaks correspond to $I_0$ current shown in Fig. 1 and equation (1). Such a voltammogram shape could originate from the possibility of the adopting by the same probe different structures, including open and zipped forms (Table 2), which in turn lead to split peaks of significant smaller current intensity and of significant broader base than in the case of other investigated probes. This significantly affected the linear relationship between cDNA concentration and the signal change, the standard deviations of the obtained results and the easiness of its interpretation.

That is why for further sensor development, only probe TOX3 was chosen as a receptor. The working parameters of the sensor with TOX3 probe, for 5 and 30 min of hybridization with HPLC purified 107 nucleotide length *tox* gene fragment, were as follows: linear detection range 0.16–2.0 μM and 13.5–60.0 nM with sensitivity of 0.24 and 12.81 $1 \cdot \mu M^{-1}$ and regression coefficients 0.980 and 0.965 respectively. As the biological analysis based on the biosensor response may be hampered by the probe desorption from the electrode surface the above parameters were defined for biosensor signal change between 10 and 90% [38,39]. However, the level of detection (defined by the equation LOD = 3σ/s, where σ is the standard deviation of the corrected blank signals measured for electrochemical biosensor and s is the slope of the calibration curve) was estimated as 20.8 nM for 5 min of hybridization and 0.5 nM for 30 min hybridization. Above investigations were performed using the square wave voltammetry (SWV) as detection technique, with frequency of 100Hz (peaks registered in higher frequencies were of similar heights [40]). This allowed to shorten the time of applied potential from 3 min, when alternate current voltammetry (ACV) was used as detection technique, to about 1 s. The sensor response (Fig. 2, SWV) both for 5 and 30 min of hybridization was smaller on average by 17% and 13.5%, respectively, than sensor response registered with the use of ACV technique (Fig. 2, ACV). However, in the point of view of the ultimate application of the proposed biosensors as a detection part of microfluidic device for real life applications, the time of the detection procedure may play a crucial role. Especially as the real asymmetric PCR product concentration, calculated at the base of intensity of

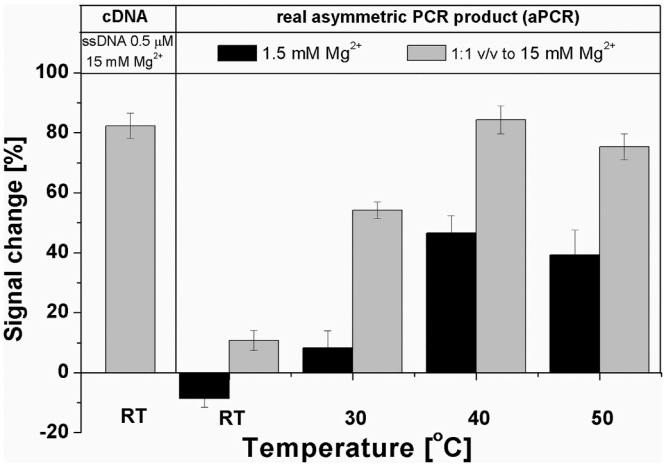


**Fig. 3.** Influence of detection temperature and magnesium ion concentration increasement on biosensor's signal change (with TOX3 as a probe) after 30 min of hybridization with real asymmetric PCR product of 107 nucleotide length *tox* gene fragment, ($n \geq 4$).

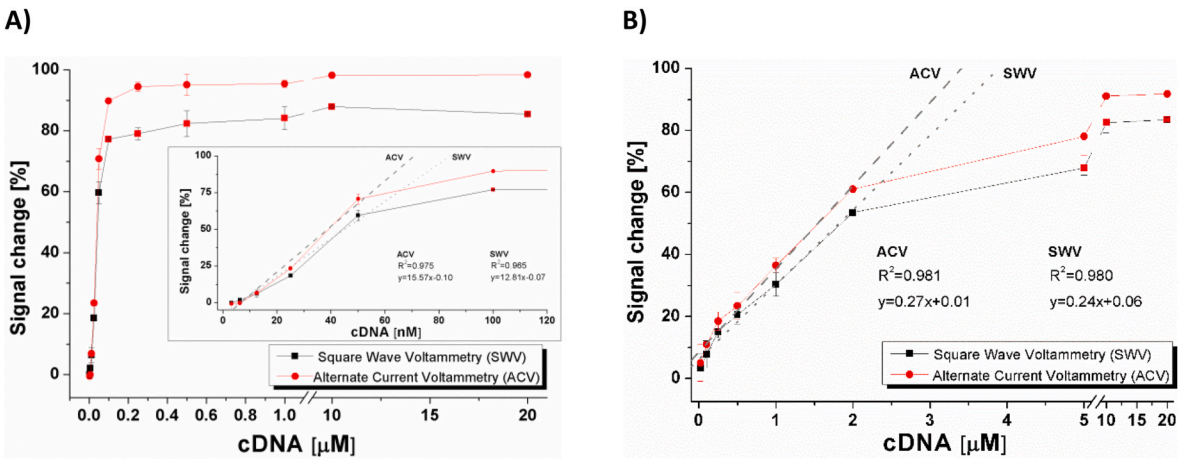


**Fig. 2.** Comparison of the detection technique used for cDNA detection with the use of biosensor with TOX3 probe for analyzed hybridization times A) 30 min and B) 5 min. Insets are provided for better view of the biosensor's response in its linear range, ($n \geq 4$).

corresponding band present on polyacrylamide gel electrophoresis (Fig. 1B-SM), was estimated at the level of about 0.54 μM. This value lies within the linear range for 5 min of hybridization and well above the linear detection range for 30 min of hybridization (Fig. 2).

### 3.2. Biological material sampling, DNA extraction and fast tox gene amplification

As was previously mentioned, the diphtheria is a potential health problem especially in resource limited areas, where the disease has the highest probability to emerge (refugee camps and developing countries [4]). That is why the simple and cost efficient genetic detection method should be also supplemented with easy and possible to perform outside laboratories DNA sampling, isolation and amplification methods. The sampling procedure was previously estimated and according to our findings the crucial for appropriate diphtheria diagnosis based on proteins investigation (diphtheria toxin) the different swab material should be used than for nucleic acids investigations [27]. Investigated by us the simplified procedures recommended for *Corynebacterium diphtheriae* DNA extraction from swabs containing bacterial cells is based on the use of magnetic beads and filter paper to capture the DNA are provided in Materials and Methods section of this manuscript. The effectiveness of the extraction was verified by PCR. The efficiency of PCR amplification of DNA extracted using both methods was compared to the DNA sample extracted with DNeazy Blood and Tissue Kit (Qiagen) as a reference method and used for quantitative results in presented manuscript. Despite significant simplification of the procedure of DNA extraction, the amount of extracted DNA was sufficient for PCR and no inhibition of the PCR was detected (results not shown). We also propose the cost efficient and field ready microflow device for fast (15 min) amplification of 107 nucleotide long *tox* gene in asymmetric PCR reaction fragment However as it is the subject of patent pending and is published elsewhere [28] herein only brief information will be provided (Fig. 2-SM). The main part of this device is a chip with a specific microchannel system in which reaction takes place (Fig. 2A-SM). The chip structure can be divided into three separate zones, which correspond to three steps of the reaction: denaturation, annealing and elongation. The chip was connected to a separately constructed miniaturized peristaltic pump and valve, which provided required flow of the reaction mixture. An external set of heaters provided adjustment of the temperature in individual zones of the chip to carry out subsequent steps of the reaction (Fig. 2B-SM). Dedicated software has been developed to control both the pump and the valve. This resulted in a modular device for carrying out PCR reactions allowing for automatic introduction of the mixture into the chip and its circulation within the chip. The adjustment of any number of reaction cycles and the flow rates of the mixture in a wide range, hence also the total reaction time, was possible in such a device (Fig. 2C-SM).

### 3.3. Detection of tox gene fragment as a product of real asymmetric PCR (aPCR)

The amplified *tox* gene fragment, real asymmetric PCR product (aPCR), was subjected to the analysis with biosensor where TOX3 probe was used (Fig. 2). However, despite the fact that such a sensor in room temperature (RT) was sensitive to HPLC purified single stranded DNA of the same sequence as *tox* gene fragment (Figs. 2 and 3, cDNA), the biosensor response registered for direct aPCR was of significantly different characteristic (Fig. 3, aPCR, RT). According to the utilized mechanism, the current registered for TOX3 probe should decrease after hybridization, or stay at the same level when no complementary strand was present in the sample. This assumption was true only when the aPCR was detected in elevated temperatures, or when it was diluted 1:1 v/v with solution of appropriate magnesium ion concentration in order to finally obtain 15 mM $Mg^{2+}$ in analyzed sample (according to results presented in Fig. 1A-SM). As could be seen, when the direct aPCR product detection was performed in room temperature the increase in the registered current could be observed, even despite the fact that no new TOX3 probes were added to the sample. Moreover, as the *tox* gene fragment concentration in aPCR was estimated at the level of 0.54 μM, the registered biosensor response in RT for undiluted aPCR sample or sample diluted 1:1 v/v to 15 mM $Mg^{2+}$, were significantly below expected values of approximately 80% for 30 min hybridization time (Figs. 2 and 3 cDNA).

Above results indicate that the proteins, indispensable for PCR reaction, present in the real sample significantly hamper the DNA/DNA recognition in room temperature. This was confirmed by the improved biosensor response after increasing the temperature (changes in DNA/proteins second order structures and the same in DNA/proteins interactions [41]). According to obtained results (Figs. 2 and 3 cDNA), the expected biosensor response (approximately 80% signal change) was obtained only for 40 °C. After further temperature increase resulted in smaller signal change most likely due to receptor layer degradation or thiols desorption from the electrode surface. However above observation proved that to successful detection of *tox* gene fragment in real samples in ambient conditions it is necessary (i) to use increased magnesium ion concentration in the sample and (ii) to reduce the DNA/proteins interactions.

To further elucidate the necessity of the magnesium ion concentration increase and the possible reason of nonspecific biosensor response (current increase after receptor layer contact with aPCR sample in room temperature), the receptor layer with significantly different electrode blocking agent was prepared. The mercaptohexanol (MCH, with partially negative –OH group) was changed into diethyldithiocarbamate (DEDTC, characterized by resonance structures and proximity to the Fermi level of gold [25]). Such a change should lead to the significant reduction in overall negative charge present at the modified electrode surface and to significant increase in its conductivity. We already proved that the resistivity of the bare gold electrode was increased from 500 Ω to 1500 Ω for MCH and reduced to 30 Ω when the gold was modified with DEDTC [25]. Although in the literature there are information about the possible substitution of the thiols, especially for pure quality monolayers, already covalently attached to the gold electrode by the DEDTC [42,43], such a phenomena was not observed for DNA probes in the presented study. The currents, of the electrochemical TOX3 probes already immobilized at the electrode surface, were registered twice, after 24h and 72h of filler immobilization (Fig. 4 A).

As could be seen, the effect of the extended blocking agent immobilization time on the registered currents is significantly different. In the case of TOX3/MCH (Fig. 4 A), the blocking agent immobilization elongation from 24h to 72h resulted in decreasement of the registered current (by 40%), what could be explained by more dense MCH layer formation (confirmed by the increase in the overall electrode resistivity) or TOX3 probe substitution at the electrode surface. The opposite results were observed for TOX3/DEDTC (Fig. 4 B). The currents registered after extended DEDTC immobilization time, related to electrochemical reaction of redox marker attached to TOX3 probe, were higher by almost 150% (with keeping quality of peaks on the registered voltammograms which could be interpreted as no unspecific adsorption of the immobilized probes took place). Such a behavior could be explained by an increase in the overall electrode conductivity by more dense DEDTC layer. The similar observation, the current increase after real aPCR product detection in room temperature was shown in Fig. 3, when the MCH was used as the electrode blocking layer. According to the literature, in certain conditions the nonspecific protein adsorption at the electrode surface also could lead to the increase in its conductivity (change in the isoelectric point at the electrode surface and the same increase in the local ion concentration) [44,45]. As further confirmed, the change in type of electrode blocking agent from MCH into DEDTC significantly affects also the requirements for cations concentration in buffer dedicated to hybridization process to take place (Fig. 4C). As was shown in Fig. 1A-SM, the most suitable buffer was composed with 15 mM $MgCl_2$,

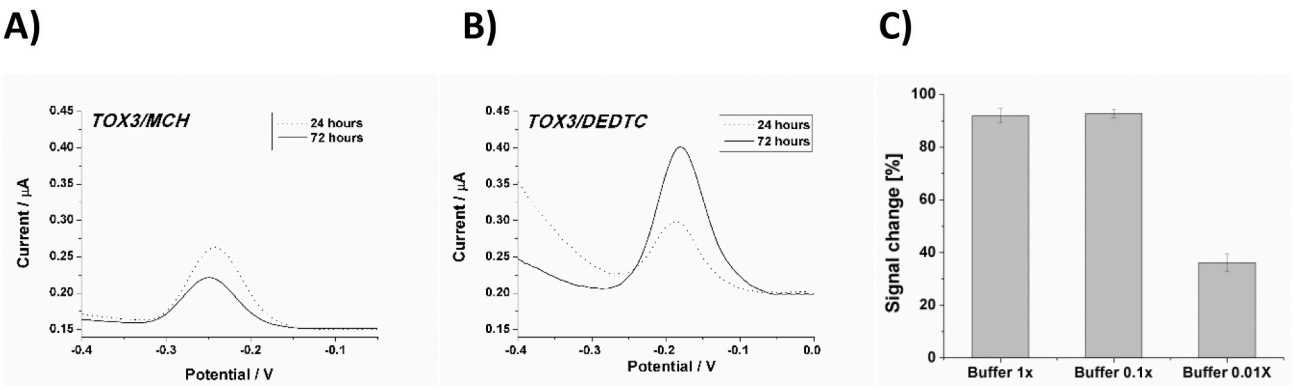


**Fig. 4.** A) and B) Influence of the blocking agent type and its immobilization time on the current registered for ready to use electrochemical biosensor of TOX3/MCH or TOX3/DEDTC receptor layer. C) response of the electrochemical biosensor with TOX3/DEDTC receptor layer for 0.2 µM HPLC purified 107 nucleotide long *tox* DNA gene fragment after 30 min of hybridization time, ($n \geq 4$). As the detection technique the SWV was used.

50 mM KCl, 10 mM Tris-HCl, pH 7 which resulted in biosensor (TOX3/MCH) response for 0.25 µM HPLC purified cDNA at the level of 79 ± 2% (Fig. 2). The potassium or magnesium concentration reduction in the buffer leads to smaller biosensor response and higher standard deviations. As was shown in Fig. 4C, Buffer 1x, the biosensor response with TOX3/DEDTC receptor layer for the same cDNA concentration and in the same buffer was at the level of 92 ± 3%. The similar result were obtained after tenfold dilution of the hybridization buffer (buffer 0.1x), 93 ± 2%. After next tenfold dilution (Buffer 0.01x; with final composition of 0.15 mM $MgCl_2$, 0.5 mM KCl, 0.1 mM Tris-HCl, pH 7) the biosensor response was reduced to 36 ± 4%. As was shown elimination from the electrode surface significant negative charge of –OH present in MCH blocking agent and substituted it with DEDTC eliminated the necessity of increased mono- or divalent cations concentration versus real aPCR product. This allows in turn, after further optimization steps, direct electrochemical detection of real asymmetric *tox* gene fragment as a PCR product, without the necessity of its dilution with appropriate ions or other compounds. This will be more intensively investigated by us in the future.

However, after ions concentration optimization the satisfactory biosensor response for aPCR product was still observed only when the temperature was elevated (Fig. 3). As the temperature increase did not influence the $I_0$ current value (used in biosensor signal change in equation (1)), most probably the interactions between aPCR product and proteins present in the sample hamper the biosensor response. Information about destabilization of proteins structure by even small addition of organic solvents to their water solutions have already been reported [46–50]. One of such, used in the presented study, dimethyl sulfoxide (DMSO), belongs to this group of solvents. According to the literature, this small amphipathic organic molecule with a hydrophilic sulfoxide group and two hydrophobic methyl groups (favorable proton acceptor than donor) influences the DNA-protein interaction at several levels [49,50]. At low concentrations, where proteins shows negative preferential DMSO binding, or preferential hydration, this solvent often is used as a cryoprotectant during the cells or proteins freezing. However, when DMSO concentration is increased, the preferential interaction changed to DMSO binding, correlated with structural changes and proteins unfolding which reduce ligand binding affinities by as much as 10-fold with just 10% DMSO participation in buffer [50,51]. It was also proved that addition of the organic solvents to buffers where nucleic acids hybridization took place (in bulk solution) increase both the hybridization efficiency and the specificity [52]. As could be seen (Fig. 5) also in our investigations, surface confined electrochemical detection of nucleic acid, the DMSO significantly improved the biosensor response in room temperature.

The analyzed sample, asymmetric aPCR product was enriched in magnesium ion (final concentration of 15 mM $Mg^{2+}$) and DMSO by addition of appropriate solution in 1:1 v/v proportion. This resulted in surface confined electrochemical detection, in room temperature, of amplified single stranded *tox* gene fragment (107 nucleotide length) of toxigenic *Corynebacterium diphtheriae* strain with the use of TOX3/MCH receptor layer. This proved that to perform this assay the negative charge deposited at the electrode surface (phosphate moieties in stem-loop probe and –OH groups of MCH) had to be screened with magnesium ion, and DNA/protein interactions had to be disrupted, in this case with dimethyl sulfoxide.

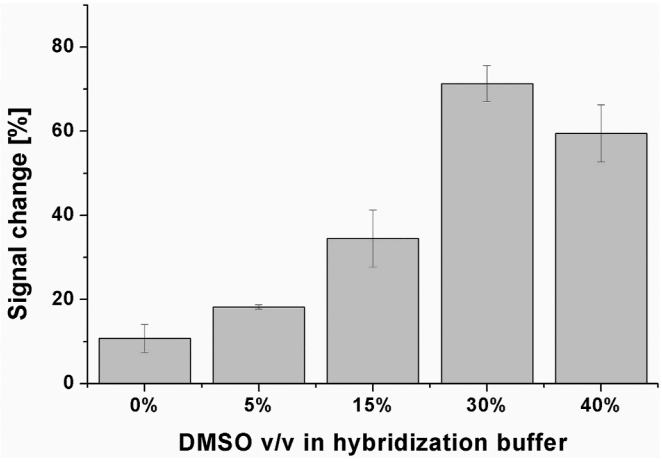


**Fig. 5.** The influence of DMSO concentration in hybridization buffer on registered biosensor response, ($n \geq 4$). The hybridization was conducted with aPCR product for 30 min.

### 3.4. Real sample analysis

Except confirmation of the developed biosensor applicability in electrochemical real aPCR product detection, also its usefulness in real life analysis was proved. Test samples were prepared, amplified in traditional and asymmetric PCR mode using primers complementary to the *tox* gene fragment encoding the diphtheria toxin gene of *Corynebacteriu diphtheriae* strains. The DNA templates were isolated from bacterial strains (Fig. 3-SM) that may occur in the human upper respiratory tract and may be a potential pathogen, including the toxin-forming strain *Corynebacterium diphtheriae* NCTC 10648, gravis, $tox^+$ (toxin-strain) and *Corynebacterium diphtheriae* 5820/2019, $tox^-$ (non-toxic strain).

The DNA matrixes composition for 107 nucleotide length *tox* gene fragment amplification are given in Fig. 3-SM. There are both single

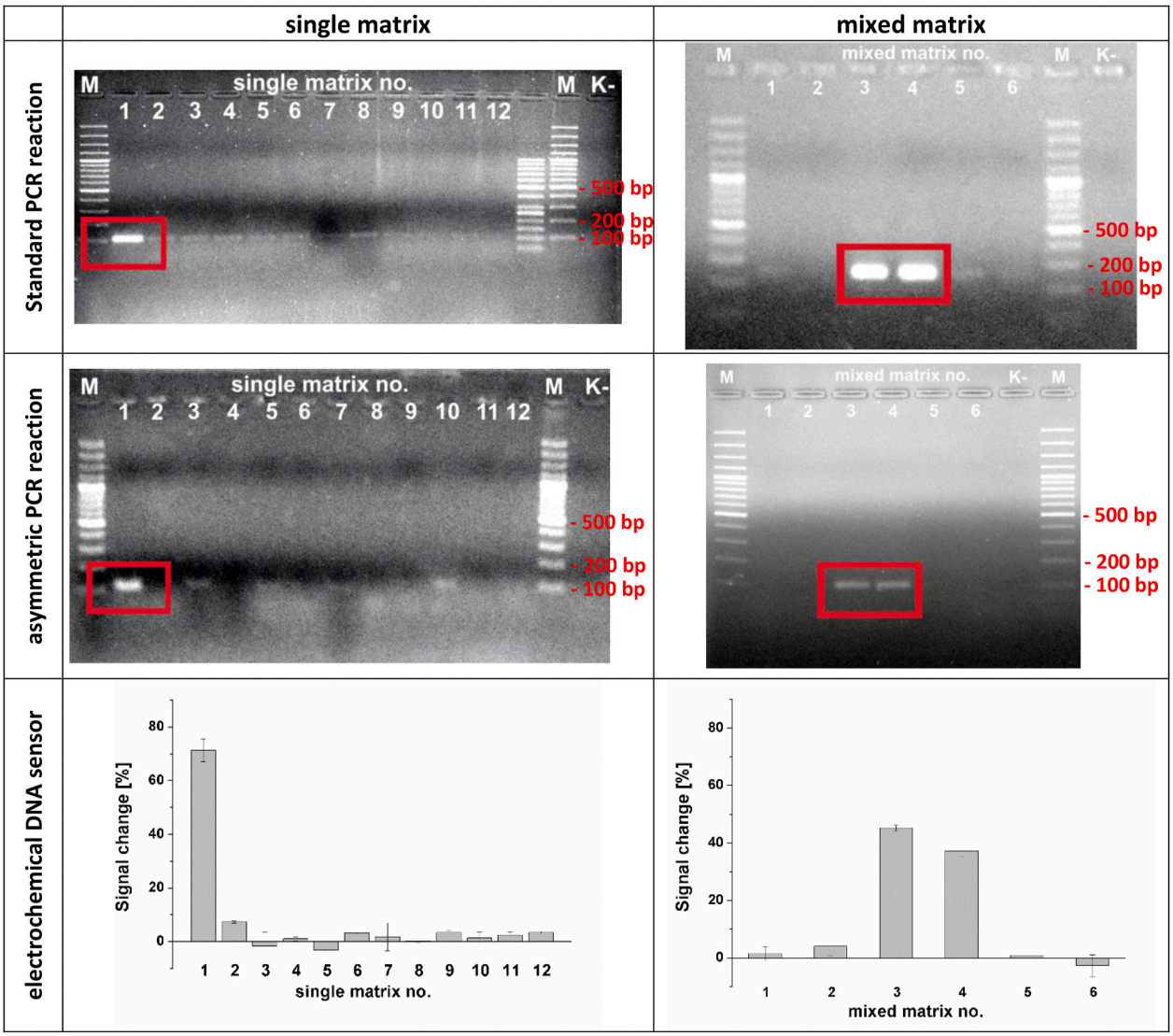


**Fig. 6.** Comparison of gel electrophoresis (standard and asymmetric PCR reaction products) and electrochemical DNA detection, $n \geq 4$, (asymmetric PCR reaction products) results after *tox* gene amplification with the use of matrixes prepared according to Fig. 3-SM. (M) – 100 bp Plus Ladder, Thermo Scientific GeneRuler; (K-) - negative control.

matrixes (Fig. 3A-SM), where only DNA isolated from a given pathogen strain DNA was subjected for further analysis, and mixes of DNA templates (Fig. 3B-SM), where DNA isolated from different pathogens were combined and subjected for further analysis. In Fig. 3C-SM also examples of chosen bacterial strains growth was given.

The specificity of the 107 nucleotide length *tox* gene fragment amplification with the use of standard (Fig. 6, Standard PCR reaction) and asymmetric (Fig. 6, asymmetric PCR reaction) PCR reaction was proved after the gel electrophoresis. The clear bands, of the appropriate length were visualized only for matrixes where the toxigenic strains of Corynebacterium diphtheria were present (single matrix no. 1 and mixed matric no. 3 and 4). The products of the asymmetric PCR reaction (after its enrichment in magnesium ion and DMSO) were subjected also to electrochemical detection by developed biosensor (Fig. 6, electrochemical DNA sensor). The results clearly confirms that the biosensor response was observed only for samples where the *tox* gene fragment was amplified. This confirmed the applicability of our sensor in real life investigations.

### 3.5. *Application of disposable electrochemical transducers in tox gene fragment detection (aPCR)*

To make the field-ready fast electrochemical genetic diphtheria diagnosis possible, it is necessary also to perform the DNA detection with a compact, easy in use and disposable transducers, capable of direct utilization in more advanced devices. We tested two classical 3-electrode electrochemical transducer for the possibility of their utilization in such an applications, AC1.W1.R2 (gold working electrode simply screen-printed on a ceramic corundum ceramic base) and AC1P.W1.R2 (high quality homogenous and polished gold surface with roughness less than 1 μm) from BVT Technologies, Czech Republic (Fig. 7, A). Both transducers consisted a Ag/AgCl g reference electrode and a gold counter electrode.

Before use both transducers had to be cleaned as the electrochemical response in 2.5 mM $K_3Fe(CN)_6/K_4Fe(CN)_6$ in 20 mM PBS, pH 7.4 solution was highly irreversible (Fig. 7 B, dashed line). From applied different procedures (e.g. ultrasonication in water and ethanol and/or electrochemical cleaning in 0.5 M $H_2SO_4$) the simple 30 s incubation in piranha solution (3:1 v/v $H_2SO_4$:$H_2O_2$) was the most appropriate (Fig. 7 B, solid line). As in both cases the transducer response before and after

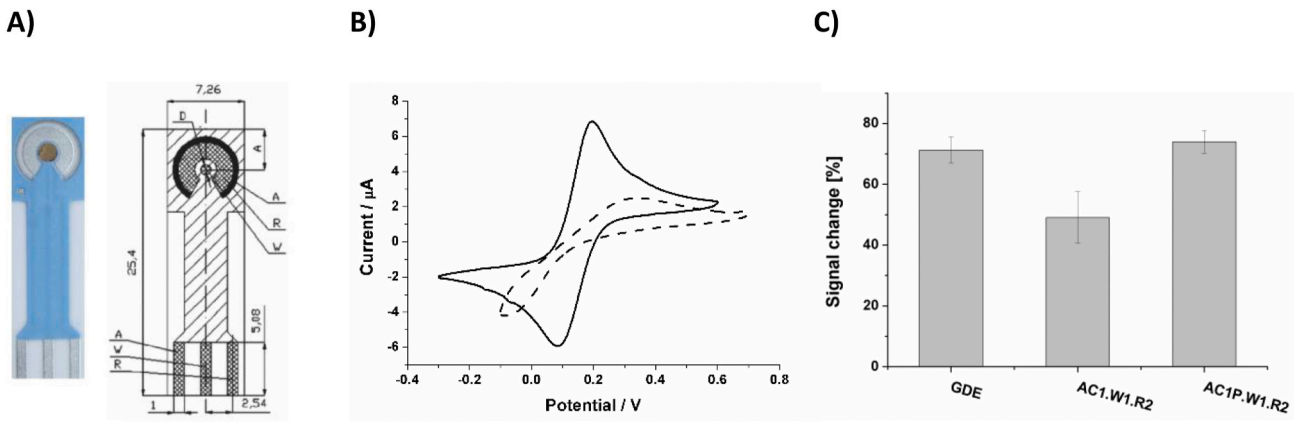


**Fig. 7.** A) Design of AC1.W1.R2 and AC1P.W1.R2 transducers (BVT Technologies, Czech Republic), **B)** effect of cleaning procedure with piranha solution: cyclic voltammetry performed in $K_3Fe(CN)_6/K_4Fe(CN)_6$ in 20 mM PBS, pH 7.4. Dashed line: before cleaning, solid line: after transducer cleaning (results shown only for AC1P.W1.R2) **C)** comparison of the biosensors response with TOX3/MCH receptor layer deposited at the gold disc electrode (GDE) and analyzed transducers AC1. W1.R2 and AC1P.W1.R2, ($n \geq 4$). (For interpretation of the references to colour in this figure legend, the reader is referred to the Web version of this article.)

cleaning was similar, only results for AC1P.W1.R2 were presented. Than the transducers were abundantly rinsed with deionized water, the biosensor receptor layer (TOX3/MCH) was prepared and the *tox* gene fragment detection performed (Fig. 7, C). As could be observed, in the case of both transducers it was possible to detect the aPCR product. However, the AC1 response significantly lower (49 ± 9%) than AC1P (74 ± 4%). Such a change most likely resulted from the difference in the above mentioned gold working electrode construction which significantly can influence the quality and composition of immobilized thiols monolayers [25]. However, the biosensor response, prepared at the AC1P transducer, was comparable to classic gold working electrode (72 ± 4%). This proves the applicability of the developed receptor layer, procedure and this transducer in modern, electrochemical genetic diphtheria diagnostic. Moreover, the compact design and ease in use of developed biosensors, together with proposed sampling [27], isolation and genetic material amplification [28] solutions make them true alternative for still valid time consuming procedures.

### 3.6. Conclusions

The presented study was dedicated to further investigations on the possibility of the application of modern, electrochemical diagnostic methods in diphtheria detection. It completes our ongoing investigations concerning the full electrochemical diagnosis of diphtheria, which also encompasses biological material sampling, electrochemical diphtheria toxoid detection, and fast amplification of tox gene fragment. As was shown, for successful electrochemical detection of the real asymmetric PCR product, it is always indispensable to optimize both the receptor structure (here as the stem-loop probe) and the assay conditions (magnesium and DMSO concentration). The origin of the initial unspecific biosensor response was elucidated and eliminated. Moreover, diethyldithiocarbamate used in the presented study for discrepancies elucidation as the new electrode blocking agent only, even in non-optimized conditions, showed a significant increase in the biosensor response towards HPLC purified cDNA. Because of these promising results, we will further investigate the possibility of its application in aPCR product detection directly in the reaction mixture. However, even the biosensor based on TOX3/MCH receptor layer allowed for highly specific and fast detection of tox gene fragment. Its detection range (calculated for signal change between 10 and 90%) was 0.16–2.0 μM (5 min hybridization) and 13.5–60.0 nM (30 min of hybridization) with respect sensitivity 0.24 and 12.81 1 $\mu M^{-1}$, regression coefficients 0.980 and 0.965 and LOD 20.8 nM and 0.5 nM. The developed biosensor proved its applicability by detection the *tox* gene fragment of *Corynebacterium diphtheriae* in the PCR samples. The selectivity was confirmed by real samples analysis where the genetic material was originated from several non-target bacterial species, which potentially can be present in the human upper respiratory tract. Moreover, the electrochemical genosensor elaborated in the presented study, based on the compact 3-electrode transducer, most probably could be directly introduced into more advanced Point-of-Care devices.

Still for pathogen detection the high-throughput, well plate-based bioanalytical techniques (e.g. ELISA) or polymerase chain reaction (PCR) are considered as gold standard which was extensively described in appropriate reviews [53–57]. The stage of an infection and the availability of antibodies and DNA sequences (viral RNA/DNA, toxin-producing genes, species and/or strain-selective genes) are factors which determine of using immunoassays or DNA-based assays in the given case. However, emerging label-free biosensors for pathogen detection and bioanalytical techniques using selective biorecognition element in combination with an analytical system are capable of being highly sensitive and robust and are becoming considered as complement to PCR and ELISA for pathogen detection. As can be found in the literature, the DNA biosensor's performance in this matter can be further improved by application of other electrode substrates or by application of other bio-electrochemical signal transduction methods. The application of self-organized monolayers in receptor layers and external redox marker for signal generation allowed for elaboration of multiple use biosensors. The obtained detection limits of such were at the level of micro to femto molar [58]. The lowest LOD were obtained for electrodes modified with conducting polymers (e.g. polyaniline) [59]. On the other hand the detection limits for biosensors where detection mechanism were using conformational changes of the redox-labelled DNA probe tethered to the electrode surface lies within the range of nano to the picomolar [58,60]. For example F. Li et al. developed biosensor with LOD at the level of 1 pM, linear detection in the range of 0.001–1 nM and sensitivity of 2.3622%·$nM^{-1}$. This parameters were obtained for the DNA detection assay time of 60 min [61].

## Author contributions

Conceptualization, methodology, R.Z. and E.M.; writing—original draft preparation, R.Z., K.M; writing—review and editing, R.Z., K.M., E. M., A.Z.; visualization, investigation R.Z., K.M., I.O., S.O., A.Z.; supervision, R.Z, E.M.; funding acquisition, R.Z. All authors have read and agreed to the published version of the manuscript.

## Declaration of competing interest

The authors declare that they have no known competing financial

interests or personal relationships that could have appeared to influence the work reported in this paper.

## Acknowledgements

This work was financially supported by the National Center for Research and Development, Poland (LIDER/35/0041/L-7/15/NCBR/2016) and by Warsaw University of Technology. We would like also to thank CEZAMAT PW for the opportunity to use the equipment.

Project implemented as part of interdisciplinary TRI-BIO-CHEM studies co-financed by the National Center for Research and Development, implemented as part of the Operational Program Knowledge Education Development 2014-2020 co-financed by the European Social Fund.

## Appendix A. Supplementary data

Supplementary data to this article can be found online at https://doi.org/10.1016/j.talanta.2021.122161.

## References

[1] J.F. Lindahl, D. Grace, The consequences of human actions on risks for infectious diseases: a review, Infect. Ecol. Epidemiol. 5 (2015) 30048.
[2] G. Verikios, J.M. McCaw, J. McVernon, A.H. Harris, H1N1 influenza and the Australian macroeconomy, JAPE 17 (2012) 22–51.
[3] A. Sharif, C. Aloui, L. Yarovaya, COVID-19 pandemic, oil prices, stock market, geopolitical risk and policy uncertainty nexus in the US economy: fresh evidence from the wavelet-based approach, Int. Rev. Financ. Anal. 70 (2020) 101496.
[4] A.A. Zasada, A. Wiatrzyk, U. Czajka, K. Brodzik, K. Formińska, E. Mosiej, M. Prygiel, K. Krysztopa-Grzybowska, K. Wdowiak, Application of loop-mediated isothermal amplification combined with colorimetric and lateral flow dipstick visualization as the potential point-of-care testing for Corynebacterium diphtheria, BMC Infect. Dis. 20 (2020) 308.
[5] E. Tambo, A.G. El-Dessouky, E.I.M. Khater, Z. Xianonng, Enhanced surveillance and response approaches for pilgrims and local Saudi populations against emerging Nipah, Zika and Ebola viral diseases outbreaks threats, J. Infect. Public Heal. 13 (2020) 674–678.
[6] A. El-Sayed, M. Kamel, Climatic changes and their role in emergence and re-emergence of diseases, Environ. Sci. Pollut. Res. 27 (2020) 22336–22352.
[7] https://www.cdc.gov/diphtheria/clinicians.html accession date:2020.03.20.
[8] W. Rastawicki, N. Rokosz-Chudziak, Characteristics and assessment of the usefulness of serological tests in the diagnostic of infections caused by coronavirus SARS-CoV-2 on the basis of available manufacturer's data and literature review, Przegl. Epidemiol. 74 (2020) 113–132.
[9] O. Pashchenko, T. Shelby, T. Banerjee, S. Santra, A comparison of optical, electrochemical, magnetic, and colorimetric point-of-care biosensors for infectious disease diagnosis, ACS Infect. Dis. 4 (2018) 1162–1178.
[10] V. Velusamy, K. Arshak, O. Korostynska, K. Oliwa, C. Adley, An overview of foodborne pathogen detection: in the perspective of biosensors, Biotechnol. Adv. 28 (2010) 232–254.
[11] M.E.E. Alahi, S.C. Mukhopadhyay, Detection methodologies for pathogen and toxins: a review, Sensors 17 (2017) 1885.
[12] D. Liu, J. Wang, L. Wu, Y. Huang, Y. Zhang, M. Zhu, Y. Wang, Z. Zhu, C. Yang, Trends in miniaturized biosensors for point-of-care testing, TrAC Trends Anal. Chem. (Reference Ed.) 122 (2020) 115701.
[13] V.N. Ataide, L.F. Mendes, L.I.L.M. Gama, W.R. De Araujo, T.R.L.C. Paixaõ, Electrochemical paper-based analytical devices: ten years of development, Anal. Methods 12 (2020) 1030–1054.
[14] A. Fernández-la-Villa, D.F. Pozo-Ayuso, M. Castaño-Álvarez, Microfluidics and electrochemistry: an emerging tandem for next-generation analytical microsystems, Curr. Opin. Electrochem. 15 (2019) 175–185.
[15] European Centre for Disease Prevention and Control (ECDC), Rapid Risk Assessment: a Fatal Case of Diphtheria in Belgium, ECDC, Stockholm, 2016, 2016a. Available from: http://ecdc.europa.eu/en/publications/Publications/RRA-Diphtheria-Belgium.pdf.
[16] T.S.P. Tiwari, Diphtheria, in: CDC Yellow Book 2018: Centers for Disease Control and Prevention, Oxfort University Press, New York, 2018.
[17] World Health Organization, Diphtheria Reported Cases, 2018. http://apps.who.int/immunization_monitoring/globalsummary/timeseries/tsincidencediphtheria.html.
[18] D.M. Meinel, R. Kuehl, R. Zbinden, V. Boskova, C. Garzoni, D. Fadini, Outbreak investigation for toxigenic Corynebacterium diphtheriae wound infections in refugees from Northeast Africa and Syria in Switzerland and Germany by whole genome sequencing, Clin. Microbiol. Infect. 22 (2016) 1003.
[19] J. Sane, T. Sorvari, M. Wideström, H. Kauma, U. Kaukoniemi, E. Tarkka, Respiratory diphtheria in an asylum seeker from Afghanistan arriving to Finland via Sweden, December 2015, Euro Surveill. 21 (2016) 14–17.
[20] C. Scheifer, C. Rolland-Debord, E. Badell, F. Reibela, A. Aubrya, A. Perignona, O. Pateyd, S. Brisse, E. Caumes, Re-emergence of Corynebacterium diphtheria, Med. Maladies Infect. 49 (2019) 463–466.
[21] I. Kantsone, I. Lucenko, J. Perevoscikovs, More than 20 years after re-emerging in the 1990s, diphtheria remains a public health problem in Latvia, Euro Surveill. 21 (2016) 30414.
[22] European Centre for Disease Prevention and Control (ECDC), Gap Analysis on Securing Diphtheria Diagnostic Capacity and Diphtheria Antitoxin Availability in the EU/EEA, ECDC, Stockholm, 2017. https://ecdc.europa.eu/sites/portal/files/documents/Diphtheria%20Gap%20Analysis%20final%20with%20cover%20for%20web.pdf.
[23] A.A. Zasada, E. Mosiej, Contemporary microbiology and identification of Corynebacteria spp. causing infections in human, Lett. Appl. Microbiol. 66 (2018) 472–483.
[24] K. Kupferschmidt, Life-saving Diphtheria drug is running out: two children's deaths in Europe spur search for new sources of antitoxin, Science 355 (2017) 118–119.
[25] R. Ziółkowski, A. Kaczmarek, I. Kośnik, E. Malinowska, Reduced nonspecific protein adsorption by application of diethyldithiocarbamate in receptor layer of diphtheria toxoid electrochemical immunosensor, Bioelectrochemistry 132 (2020) 107415.
[26] R. Ziółkowski, M. Jarczewska, M. Drozd, A.A. Zasada, E. Malinowska, Studies on the development of electrochemical immunosensor for detection of diphtheria toxoid, J. Electrochem. Soc. 166 (2019) B472–B481.
[27] A.A. Zasada, K. Zacharczuk, K. Woźnica, R. Ziółkowski, E. Malinowska, The influence of a swab type on the results of point-of-care tests, Amb. Express 10 (2020) 46.
[28] K. Marchlewicz, R. Ziółkowski, K. Żukowski, E. Malinowska, A Miniaturized Device for Performing PCR, Integrated with an Electrochemical DNA Biosensor for Detection of Corynebacterium Diphtheriae. 2020 Meet. Abstr. MA2020-01 1945. DOI: https://doi.org/10.1149/MA2020-01271945mtgabs.
[29] J. Kehrmann, W. Popp, B. Delgermaa, J. Buer, N. Tsogbadrakh, Two fatal cases of plague after consumption of raw marmot organs, Emerg. Microb. Infect. 9 (2020) 1878–1880.
[30] E.E. Ferapontova, Hybridization biosensors relying on electrical properties of Nucleic Acids, Electroanal. 29 (2017) 6–13.
[31] A. Abi, E.E. Ferapontova, Electroanalysis of single-nucleotide polymorphism by hairpin DNA architectures, Anal. Bioanal. Chem. 405 (2013) 3693.
[32] R. Ziółkowski, S. Oszwałdowski, K. Zacharczuk, A.A. Zasada, E. Malinowska, Electrochemical detection of bacillus anthracis protective antigen gene using DNA biosensor based on stem-loop probe, J. Electrochem. Soc. 165 (2018) B187–B195.
[33] A. Tsourkas, M.A. Behlke, S.D. Rose, G. Bao, Hybridization kinetics and thermodynamics of molecular beacons, Nucleic Acids Res. 31 (2003) 1319.
[34] S. Tyagi, F.R. Kramer, Molecular beacons: probes that fluoresce upon hybridization, Nat. Biotechnol. 14 (1996) 303.
[35] A. Chenal, P. Nizard, D.J. Gillet, Structure and function of diphtheria toxin: from pathology to engineering, Toxicol.-Toxin. Rev. 21 (2002) 321–358.
[36] https://eu.idtdna.com/site/account/login?returnurl=%2Fcalc%2Fanalyzer.
[37] T. Špringer, H. Šípová, H. Vaisocherová, J. Štepánek, J. Homola, Shielding effect of monovalent and divalent cations on solid-phase DNA hybridization: surface plasmon resonance biosensor study, Nucleic Acids Res. 38 (2010) 7343–7351.
[38] D. Kang, A. Valléee-Bélisle, A. Porchetta, K.W. Plaxco, F. Ricci, Re-engineering electrochemical biosensors to narrow or extend their useful dynamic range, Angew. Chem. Int. Ed. 51 (2012) 6717.
[39] A. Goldbeter, D.E. Koshland, An amplified sensitivity arising from covalent modification in biological systems, Proc. Natl. Acad. Sci. U.S.A. 78 (1981) 6840.
[40] W. Yang, R.Y. Lai, Comparison of the stem-loop and linear probe-based electrochemical DNA sensors by alternating current voltammetry and cyclic voltammetry, Langmuir 27 (2011) 14669–14677.
[41] R.P.C. Driessen, G. Sitters, N. Laurens, G.F. Moolenaar, G.J.L. Wuite, N. Goosen, R. T. Dame, Effect of temperature on the intrinsic flexibility of DNA and its interaction with architectural proteins, Biochemistry 53 (2014) 6430–6438.
[42] A.F. Raigoza, G. Kolettis, T.E.S. Brandt, G. Caponigri-Guerra, C. Agostino, S. A. Kandel, Coadsorption of octanethiol and dialkyldithiocarbamate on Au(111), J. Phys. Chem. C 116 (2012) 1930–1934.
[43] A.F. Raigoza, G. Kolettis, D.A. Villalba, S.A. Kandel, Restructuring of octanethiolate and dialkyldithiocarbamate monolayers in the formation of sequentially adsorbed mixed monolayers, J. Phys. Chem. C 115 (2011) 20274–20281.
[44] H. Trzeciakiewicz, J. Esteves-Villanueva, R. Soudy, K. Kaur, S. Martic-Milne, Electrochemical characterization of protein adsorption onto YNGRT-Au and VLGXE-Au surfaces, Sensors 15 (2015) 19429–19442.
[45] J. Lum, R. Wang, B. Hargis, S. Tung, W. Bottje, H. Lu, Y. Li, An impedance aptasensor with microfluidic chips for specific detection of H5N1 avian influenza virus, Sensors 15 (2015) 18565–18578.
[46] J.A. Schellman, Protein stability in mixed solvents: a balance of contact interaction and excluded volume, Biophys. J. 85 (2003) 108–125.
[47] T. Arakawa, Protein-solvent interaction, Biophys. Rev. 10 (2018) 203–208.
[48] T.O. Street, N. Courtemanche, D. Barrick, Protein folding and stability using denaturants, Methods Cell Biol. 84 (2008) 295–325.
[49] S. Tunçer, R. Gurbanov, I. Sheraj, O. Esenturk, S. Banerjee, Low dose dimethyl sulfoxide driven gross molecular changes have the potential to interfere with various cellular processes, Sci. Rep. 8 (2018) 14828.
[50] T. Arakawa, Y. Kita, S.N. Timasheff, Protein precipitation and denaturation by dimethyl sulfoxide, Biophys. Chem. 131 (2007) 62–70.
[51] J. Lee, C.E. Vogt, M. McBrairty, H.M. Al-Hashimi, Influence of dimethylsulfoxide on RNA structure and ligand binding, Anal. Chem. 85 (2013) 9692–9698.

[52] N. Dave, J. Liu, Fast molecular beacon hybridization in organic solvents with improved target specificity, J. Phys. Chem. B 114 (2010) 15694–15699.
[53] E.E.M. Alahi, C.S. Mukhopadhyay, Detection methodologies for pathogen and toxins: a review, Sensors 17 (2017) 1885.
[54] O. Lazcka, F.J. Del Campo, F.X. Munoz, Pathogen detection: a perspective of traditional methods and biosensors, Biosens. Bioelectron. 22 (2007) 1205–1217.
[55] M. Zourob, S. Elwary, A.P. Turner, Principles of Bacterial Detection: Biosensors, Recognition Receptors and Microsystems, Springer-Verlag, New York, 2008.
[56] D. Klein, Quantification using real-time PCR technology: applications and limitations, Trends Mol. Med. 8 (2002) 257–260.
[57] B. Malorny, P.T. Tassios, P. Rådström, N. Cook, M. Wagner, J. Hoorfar, Standardization of diagnostic PCR for the detection of foodborne pathogens, Int. J. Food Microbiol. 83 (2003) 39–48.
[58] M. Lazerges, F. Bedioui, Analysis of the evolution of the detection limits of electrochemical DNA biosensors, Anal. Bioanal. Chem. 405 (2013) 3705–3714.
[59] H. Chang, Y. Yuan, N. Shi, Y. Guan, Electrochemical DNA biosensor based on conducting polyaniline nanotube Array, Anal. Chem. 79 (2007) 5111–5115.
[60] T.H. Ho, F.X. Guillon, P. Bigey, F. Bediou, M. Lazerges, Analysis of the evolution of the detection limits of electrochemical nucleic acid biosensors II, Anal. Bioanal. Chem. 409 (2017) 4335–4352.
[61] F. Li, Y. Xu, X. Yu, Z. Yu, H. Ji, Y. Songa, H. Yana, G. Zhang, Effect of the duplex length on the sensing performance of a displacement-based electrochemical nucleic acid sensor with an adjustable point mutation discrimination function, Sensor. Actuator. B Chem. 234 (2016) 648–657.